International Journal of Electrical, Electronic and Communication Sciences
ISSN: 2517-9438
Vol:7, No:12, 2013

Modelling of Induction Motor Including Skew Effect Using MWFA for Performance Improvement

M. Harir, A. Bendiabdellah, A. Chaouch, N. Benouzza

***Abstract*—**This paper deals with the modelling and simulation of the squirrel cage induction motor by taking into account all space harmonic components as well as the introduction of the bars skew in the calculation of the linear evolution of the magnetomotive force (MMF) between the slots extremities. The model used is based on multiple coupled circuits and the modified winding function approach (MWFA). The effect of skewing is included in the calculation of motors inductances with an axial asymmetry in the rotor. The simulation results in both time and spectral domains show the effectiveness and merits of the model and the error that may be caused if the skew of the bars are neglected.

***Keywords*—**Modelling, MWFA, Skew effect, Squirrel cage induction motor, Spectral domain.

I. Introduction

TODAY squirrel cage induction motors are widely used in variable speed industrial drives, so that the speed control, the optimal design and the faults diagnosis of these motors are very important [1]-[7]. For example, as most diagnostic methods make use of the spectral domain analysis for more information on faults diagnosis, authors [8]-[10] tend therefore to move towards the introduction of the skew of bar in their motors modelling and analysis in order to obtain less polluted and clear spectra.

Skew is applied to electrical machines in order to reduce undesirable effects such as cogging torques, higher-harmonic air-gap fields, torque ripple, vibrations and noise. The squirrel cage of an induction machine is skewed as to filter out the first significant field harmonics due to the slotting of the machine. The skewing of induction motors induces an electrical field in the azimuthally direction, which can lead to additional currents, if the rotor bars are not sufficiently insulated with respect to the lamination.

Several authors take this skew effect in his model according to the application to be used on one hand and the way the inductance variation is to be taken into account on the other hand. Simulation of induction motors with skew effects, using a 2-D time stepping finite element method (FEM) has been developed [11]. The 2-D FEM equations of each slice are then coupled together and solved simultaneously for further refinement by authors in [12]. To consider the inter-bar currents in the skewed rotor bars, a multi-slice-network-coupled FEM has also been proposed [13]. However, in all these formulations the axial length of each slice along the motor axis has to be equal. G. Barakat [14] has also analysed the effect of the static eccentricity including the effect of the skewed slots of the rotor and the stator in the permeance function obtained by means of simulation using FEM.

In this paper, the dynamic performance of the squirrel cage motor has been calculated by considering the various stator and rotor magnetizing inductances as well as the mutual inductances between the stator phases as variables (not constants). The variation due to the skew of the bar is taken into account by the axial asymmetry in the rotor, thus using the modified winding function approach (MWFA) for our motor modelling. The simulation results obtained illustrate; in both time and spectral domains; the effectiveness of the model and point out to the necessity of considering skew effects in some applications particularly those related to faults diagnosis in induction squirrel cage motors.

II. The Squirrel Cage Induction Motor Model

Consider an induction motor having m stator circuits and n rotor bars. The cage can be viewed as n identical and equally spaced rotor loops [2]. Voltage equations for the motor can be written in vector-matrix form as follows:

$$[V_s] = R_s \left[I_s + \frac{d[\Psi_s]}{dt} \right] \quad (1)$$

$$[V_r] = R_r \left[I_r + \frac{d[\Psi_r]}{dt} \right] \quad (2)$$

where

$$[V_s] = \left[v_1^s \; v_2^s \ldots v_m^s \right]^T, \; [V_r] = [0 \; 0 \ldots 0]^T \quad (3)$$

$$[I_s] = \left[i_1^s \; i_2^s \ldots i_m^s \right]^T, \; [I_r] = \left[i_1^r \; i_2^r \ldots i_n^r \right]^T \quad (4)$$

and the stator and rotor flux linkages are given by

$$[\Psi_s] = [L_{ss}][I_s] + [L_{sr} \; I_r] \quad (5)$$

$$[\Psi_r] = [L_{rr}][I_r] + [L_{rs} \; I_s] \quad (6)$$

L_{ss} is an m*m matrix with the stator self and mutual inductances, L_{rr} is an n*n matrix with the rotor self and mutual

M. Harir, A. Bendiabdellah, N. Benouzza are with the Diagnosis Group, L.D.E.E Laboratory, Department of Electrical Engineering, Faculty of Electrical Engineering, University of Sciences and Technology of Oran, Algeria (corresponding author to e-mail: bendiazz@yahoo.fr).

A. Chaouch is with the Signals and Systems Laboratory, Department of Electrical Engineering, Faculty of Sciences and Technology, University of Mostaganem, Algeria (e-mail: ikchaouchdz@yahoo.fr).

inductances, L_{sr} is an m*n matrix composed by the mutual inductances between the stator phases and the rotor loops, L_{rs} is an n*m matrix composed by the mutual inductances between the rotor loops and the stator phases and $L_{sr} = L_{rs}^{t}$.

The mechanical equations for the machine are

$$J\frac{d\omega_r}{dt} + T_L = T_e \tag{7}$$

$$\frac{d\theta_r}{dt} = \omega_r \tag{8}$$

where θ_r is the rotor position, ω is the angular speed, J is the rotor-load inertia and T_L is the load torque. The machine electromagnetic torque T_e can be obtained from the magnetic co-energy as:

$$T_e = \left[\frac{\partial W_{co}}{\partial \theta_r}\right]_{(I_s, I_r)} \tag{9}$$

The magnetic co-energy is the energy stored in the magnetic circuits and can be written as:

$$W_{co} = \frac{1}{2}\left[I_s^t L_{ss} I_s + I_s^t L_{sr} I_r + I_r^t L_{rs} I_s + I_r^t L_{rr} I_r\right] \tag{10}$$

The precise knowledge of the inductances making up the matrices in (5) and (6) is essential for the analysis and simulation of the motor. In the next section a method for the calculation of such inductances while taking into account the skewing of rotor bars is being presented.

III. The Inductances Calculation

All obtained inductances of the system, are calculated by using the MWFA) [15]. If we consider the modified winding function given by the following expression:

$$N(\varphi,\theta_r) = n(\varphi,\theta_r) - \frac{1}{2\pi\langle g^{-1}(\varphi,\theta_r)\rangle}\int_0^{2\pi} n(\varphi,\theta_r) g^{-1}(\varphi,\theta_r) d\varphi \tag{11}$$

From (11) and by carrying out the variable change $\varphi = x/r$ and $\theta_r = x_r/r$, This is equivalent as if one referred to an X-Z axes orthonormal reference, as shown in Fig. 1, where it is possible to imagine a planar representation of the machine. It is clear that *x*, in this case, correctly represents a linear displacement along the arc corresponding to the angular opening 'φ' and similarly for the case of x_r [5].

Knowing that *N* is the MMF per unit current, the flux seen by the turns of a coil due to the current through another coil is given by the expression:

$$\phi_{BjAi} = \mu_0 \int_0^{2\pi r}\int_0^{l} N_{Ai}(x,z,x_r) n_{Bj}(x,z,x_r) g^{-1}(x,z,x_r) r_{Ai} dz dx \tag{12}$$

The inductance between any two coils will be:

$$L_{BjA_i}(x_r) = \mu_0 \int_0^{2\pi r}\int_0^{l} N_{A_i}(x,z,x_r) n_{Bj}(x,z,x_r) g^{-1}(x,z,x_r) dz dx \tag{13}$$

In order to design for subroutines to calculate for the various inductances of the machine, it is then possible to derive a new expression that may be easier to be translated into algorithm. Let us put $P = g^{-1}(x,z,x_r)$, defined as the air gap permeance. In this case, the expression (13) of the mutual inductance can be rewritten as follows:

$$L_{BjAi}(x_r) = \mu_0 \int_0^{2\pi r}\int_0^{l} P\left(n_{Ai}(x,z,x_r) - \frac{\langle Pn_{Ai}\rangle}{\langle P\rangle}\right) n_{Bj}(x,z,x_r) dz dx \tag{14}$$

$$L_{BjAi}(x,z,x_r) = 2\pi r l \mu_0 \langle p n_{Ai} n_{Bj}\rangle - 2\pi r l \mu_0 \frac{\langle Pn_{Ai}\rangle\langle Pn_{Bj}\rangle}{\langle P\rangle} \tag{15}$$

Knowing that $n_{Ai}(x, z, x_r)$ is the distribution function of coil A_i of winding *A*, and $n_{Bj}(x, z, x_r)$ is the distribution function of a rotor mesh [4]. In the same way as in [6], and according to the type of connection between the coils, the inductance is obtained by the sum of all mutual inductances between p and q winding coils *A* and *B*, respectively [7]-[9].

$$L_{BA}(x,z,x_r) = 2\pi r l \mu_0 \left(\left(\sum_{i=1}^{q}\sum_{j=1}^{p}\langle p n_{Ai} n_{Bj}\rangle\right) - \frac{\langle Pn_A\rangle\langle Pn_B\rangle}{\langle P\rangle}\right) \tag{16}$$

$$\langle Pn_{Ai} n_{rj}\rangle = \frac{1}{2\pi r \lg_0}\int_0^{2\pi r}\int_0^{l} n_{Ai}(x,z,x_r) n_{rj}(x,z,x_r) dz dx \tag{17}$$

$$\langle Pn_{Ai} n_{rj}\rangle = \frac{1}{2\pi r \lg_0}\int_{x_{1j}}^{x_{2j}}\int_{z_{1j}(x)}^{z_{2j}(x)} n_{Ai}(x,z,x_r) n_{rj}(x,z,x_r) dz dx \tag{18}$$

which gives:

$$L_{BA}(x_r) = \sum_{i=1}^{q}\sum_{j=1}^{p} \pm L_{BjAi}(x_r) \tag{19}$$

A. Inductance Calculation without Skewing Bars

$$n_{Ai}(x,z,x_r) = \begin{cases} N_s & x_{1i} < x < x_{2i},\ 0 < z(x) < l \\ 0 & \text{in the remaining interval} \end{cases} \tag{20}$$

$$n_{rj}(x,z,x_r) = \begin{cases} 1 & x_{1j} < x < x_{2j},\ 0 < z(x) < l \\ 0 & \text{in the remaining interval} \end{cases} \tag{21}$$

Analytical integration gives us the results consigned in Table I. For each given interval, there is a value of the mutual inductance which depends on θ_r.

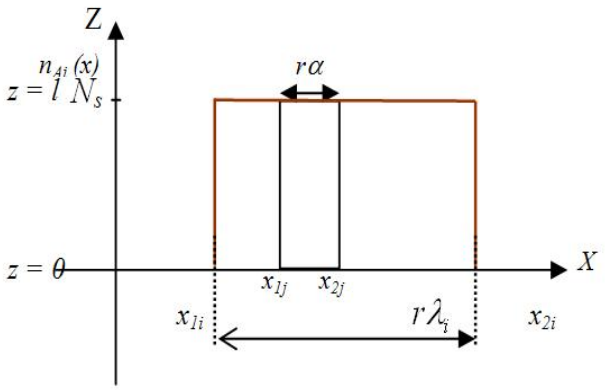

Fig. 1 Distribution function of the stator coil A_i

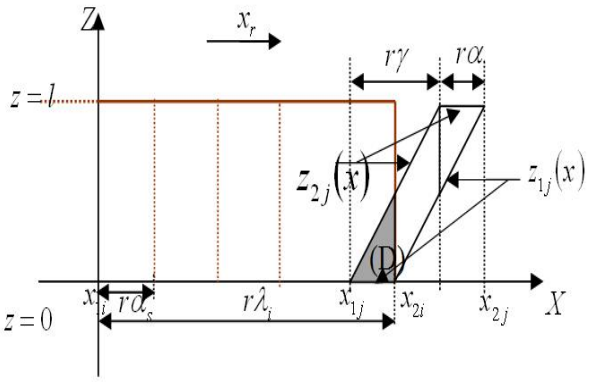

Fig. 2 Skewing bar presentation

TABLE I
MUTUAL INDUCTANCE WITHOUT SKEWING BARS

θ_r (rad)	$L_{a_i r}$ (H)
$0 \le \theta_r < \theta_{i1} - \alpha_r$	$-2\frac{\mu_0 rl}{g_0} N_s \alpha_r$
$\theta_{i1} - \alpha_r \le \theta_r < \theta_{i1}$	$\frac{\mu_0 rl}{g_0} N_s (\theta_r - \theta_{i1} - \alpha_r)$
$\theta_{i1} \le \theta_r < \theta_{i2} - \alpha_r$	$-\frac{\mu_0 rl}{g_0} N_s \alpha_r$
$\theta_{i2} - \alpha_r \le \theta_r < \theta_{i2}$	$\frac{\mu_0 rl}{g_0} N_s (-\theta_r + \theta_{i2} - 2\alpha_r)$
$\theta_{i2} \le \theta_r < 2\pi$	$-2\frac{\mu_0 rl}{g_0} N_s \alpha_r$

B. Inductance Calculation with Skewing Bars

It is assumed that the machine always has a uniform gap, but having an axial asymmetry in the rotor translated by skewing bars. Knowing that the distribution functions in Fig. 2 can be defined in two dimensions as follows:

$$n_{Ai}(x,z,x_r) = \begin{cases} N_s & x_{1i} < x < x_{2i}, 0 < z(x) < l \\ 0 & \text{in the remaining interval} \end{cases} \quad (22)$$

$$n_{rj}(x,z,x_r) = \begin{cases} 1 & x_{1j} < x < x_{2j}, z_{1j}(x) < z(x) < z_{2j}(x) \\ 0 & \text{in the remaining interval} \end{cases} \quad (23)$$

with

$$z_{1j}(x) = \begin{cases} 0 & , x_{1j} \le x \le x_{1j} + r\alpha \\ \frac{l}{r\gamma}(x - x_{1j} - r\alpha), & x_{1j} \le x \le x_{2j} \end{cases} \quad (24)$$

$$z_{2j}(x) = \begin{cases} \frac{l}{r\gamma}(x - x_{1j}), & x_{1j} \le x \le x_{1j} + r\gamma \\ 0 & , x_{1j} + r\gamma \le x \le x_{2j} \end{cases} \quad (25)$$

Such that γ is the angle of skew of the bars, and $\lambda_i = (x_{2i} - x_{1i})/r$ represents the opening of the stator coil phase. When the mesh is partially in the field of the coil, the range of integration is reduced to the common area 'D' between the projection surface of the rotor mesh and that of the coil (the gray portion of Fig. 2). Referring to (22) and (23), it is clear that the integral in the remaining field is zero.

The analytical integration gives us the mutual inductance between a stator coil and a rotor mesh. The results are illustrated in Table II. After the analytical calculation of the mutual inductance between all coils of a stator phase with a rotor mesh, we can plot their forms. In Fig. 3 (a), we can see the shape of $L_{r1A}(\theta_r)$ which is far from a sinusoid. It should be noted also that an analytical calculation of the first derivative of $L_{r1A}(\theta_r)$ (in red color) may lead to a discontinuous function. While in Fig. 3 (b), we can see the effect caused by the inclusion of skewing bars. These effects occur in a sensible change in the form of the mutual inductance, and hence a clear change in its first derivative, particularly in terms of its form rather than in terms of its maximum value.

TABLE II
MUTUAL INDUCTANCE WITH SKEWING BARS

θ_r (rad)	$L_{a_i r}$ (H)
$0 \le \theta_r < \theta_{i1} - (\gamma + \alpha_r)$	$-2\frac{\mu_0 rl}{g_0} N_s \alpha_r$
$\theta_{i1} - (\gamma + \alpha_r) \le \theta_r < \theta_{i1} - \gamma$	$\frac{\mu_0 rl}{2\gamma g_0} N_s \left[(\theta_r + \gamma + \alpha_r)^2 - {\theta_{i1}}^2 - 2\theta_{i1}(\theta_r - \theta_{i1} + \gamma + \alpha_r) - 4\alpha_r \gamma \right]$
$\theta_{i1} - \gamma \le \theta_r < \theta_{i1} - \alpha_r$	$\frac{\mu_0 rl \alpha_r}{\gamma g_0} N_s \left(\theta_r - \theta_{i1} + \frac{\alpha_r}{2} - \gamma \right)$
$\theta_{i1} - \alpha_r \le \theta_r < \theta_{i1}$	$\frac{\mu_0 rl}{\gamma g_0} N_s \left[\frac{-\left((\theta_r + \alpha_r)^2 - {\theta_{i1}}^2 \right)}{2} + (\theta_{i1} + \alpha_r)(\theta_r - \theta_{i1} + \alpha_r) - \alpha_r \left(\gamma + \frac{\alpha_r}{2} \right) \right]$
$\theta_{i1} \le \theta_r < \theta_{i2} - (\gamma + \alpha_r)$	$-\frac{\mu_0 rl}{g_0} N_s \alpha_r$
$\theta_{i2} - (\gamma + \alpha_r) \le \theta_r < \theta_{i2} - \gamma$	$\frac{\mu_0 rl}{\gamma g_0} N_s \left[\frac{\left({\theta_{i2}}^2 - (\theta_r + \alpha_r)^2 \right)}{2} + (\alpha_r - \theta_{i2})(-\theta_r + \theta_{i2} - \alpha_r) - \alpha_r \left(\gamma + \frac{\alpha_r}{2} \right) \right]$
$\theta_{i2} - \gamma \le \theta_r < \theta_{i2} - \alpha_r$	$\frac{\mu_0 rl \alpha_r}{\gamma g_0} N_s \left(-\theta_r + \theta_{i2} - \frac{\alpha_r}{2} - 2\gamma \right)$
$\theta_{i2} - \alpha_r \le \theta_r < \theta_{i2}$	$-\frac{\mu_0 rl}{\gamma g_0} N_s \left[\frac{\left({\theta_{i2}}^2 - {\theta_r}^2 \right)}{2} - \theta_{i2}(-\theta_r + \theta_{i2}) + 2\gamma \alpha_r \right]$
$\theta_{i2} \le \theta_r < 2\pi$	$-2\frac{\mu_0 rl}{g_0} N_s \alpha_r$

IV. SIMULATIONS RESULTS

Once the squirrel cage induction motor model was obtained, a simulation program written in Matlab language was then developed. The proposed program enables us to highlight the behavior of a squirrel cage induction motor in both time and spectral representations and to compare its performance for both cases that is with and without considering the bars skew effects.

A. Time Domain

The simulation model of the induction motor in the time domain gives us the electromagnetic torque curves shown in Figs. 4 (a), (b) and the stator currents in Figs. 5 (a), (b). From these curves, it can be easily noticed the improvements brought by the bars skewing, in terms of peaks reduction in the transient mode and oscillations reduction in the start-up and steady state conditions. On the other hand, the steady state current fluctuations are less important with the introduction of the skewing bars effects and the shape of its waveforms is more sinusoidal.

B. Spectral Domain

The simulation model of the induction motor in the spectral domain gives us the stator current spectra without skew effect consideration, shown in Figs. 6 (a), (b) and the stator current spectra with skew effect consideration, shown in Figs. 7 (a), (b). From these spectra, it can be easily noticed the improvements brought by the bars skewing, in terms of peaks reduction in the stator current spectra compared to the stator current spectra without skew effect consideration. Note that, for the case of our simulation without skew effect, using the FFT analysis, the rotor slot harmonics occur at frequencies:

$$f_{h1} = (17 - 18s) f = 842.35hz$$
$$f_{h2} = (19 - 18s) f = 942.35hz$$
$$f_{h3} = (35 - 36s) f = 1734.7hz$$
$$f_{h4} = (37 - 36s) f = 1834.7hz$$
$$f_{h5} = (53 - 54s) f = 2627.05hz$$
$$f_{h6} = (55 - 54s) f = 2727.05hz$$

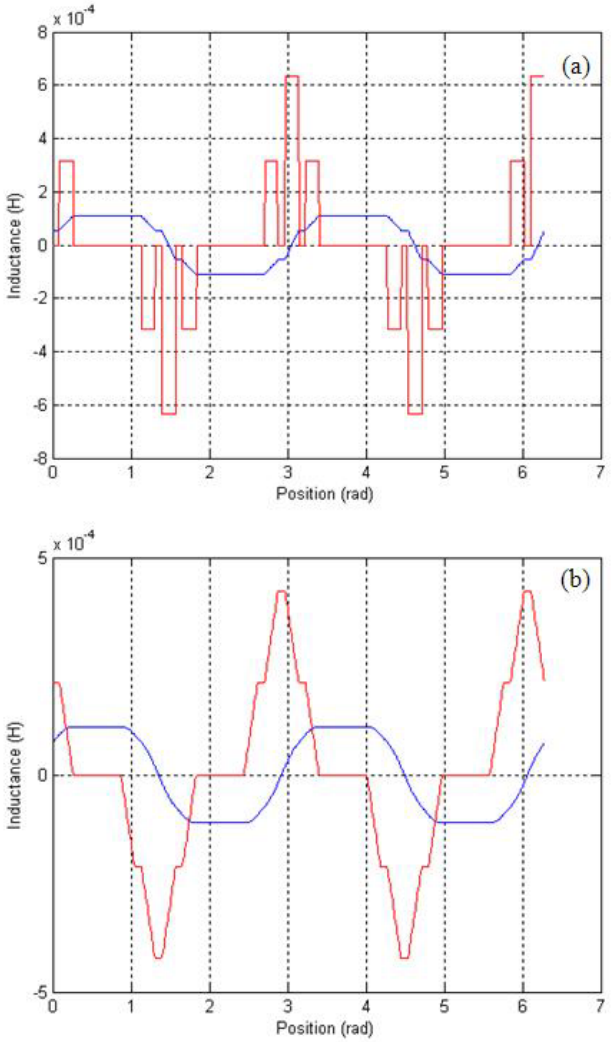

Fig. 3 Mutual inductance between the stator phase A and rotor mesh r1 (blue) and its first derivative with respect to θ_r (red) (a) without skew, (b) with skew

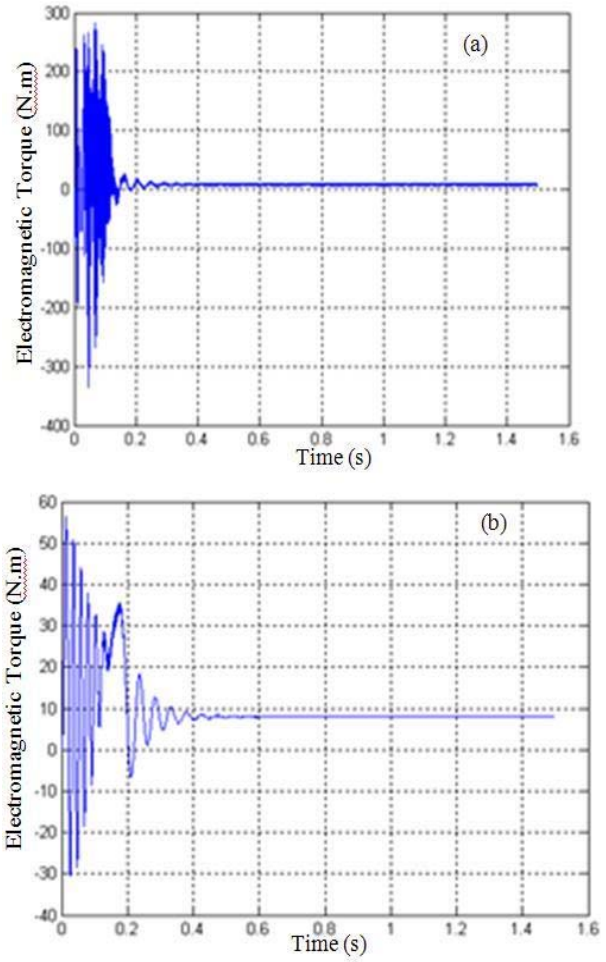

Fig. 4 Electromagnetic torque, (a) without skew, (b) with skew

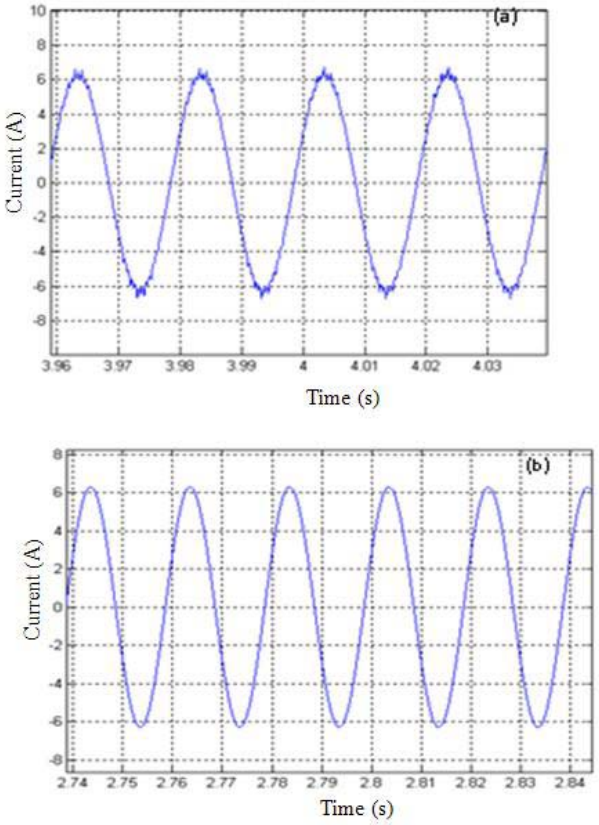

Fig. 5 Current of stator phase (a) without skew, (b) with skew

Also note that, for the case of our simulation with skew effect, the spectra are improved by indicating attenuation peaks with a small offset due to increased slip, which means an improvement of current, torque and speed. The rotor slot harmonics occur at frequencies:

$$f_{h1} = (17 - 18s) f = 839.89hz$$
$$f_{h2} = (19 - 18s) f = 939.89hz$$
$$f_{h3} = (35 - 36s) f = 1729.8hz$$
$$f_{h4} = (37 - 36s) f = 1829.8hz$$
$$f_{h5} = (53 - 54s) f = 2619.6hz$$
$$f_{h6} = (55 - 54s) f = 2719.6hz$$

V. Conclusion

In this paper, a proposed model of a squirrel cage induction motor is being presented. To take into account some of the secondary effects existing in a real motor, the model has included these effects by firstly considering all space harmonics due to the non-sinusoidal distribution of the air gap MMF and secondly all the effects produced by the skewing of bars as in our case.

The simulation results obtained, enabled us to compare the motor performance for both cases; that is; with and without skewing effects and showed us clearly the effectiveness and merits of including skew effect in the model. Both time and spectral domains are been presented. The spectral domain analysis is particularly interesting for applications related to fault diagnosis of motors where the spectrum should be less polluted to easily locate the harmonics characterizing faults in the stator current spectrum.

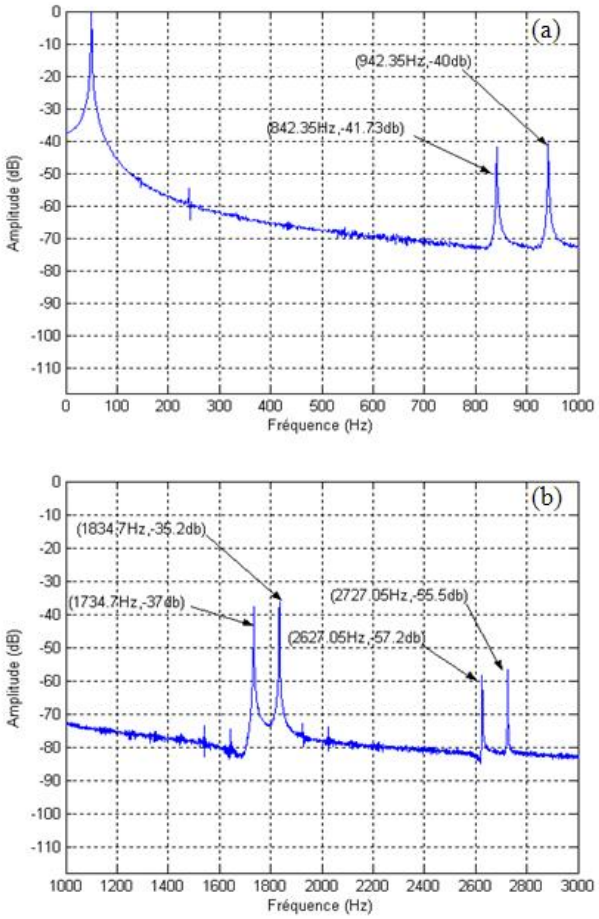

Fig. 6 The phase A stator current spectrum without taking into account the inclination of the bars, (a) for low frequencies order, (b) for high frequencies order

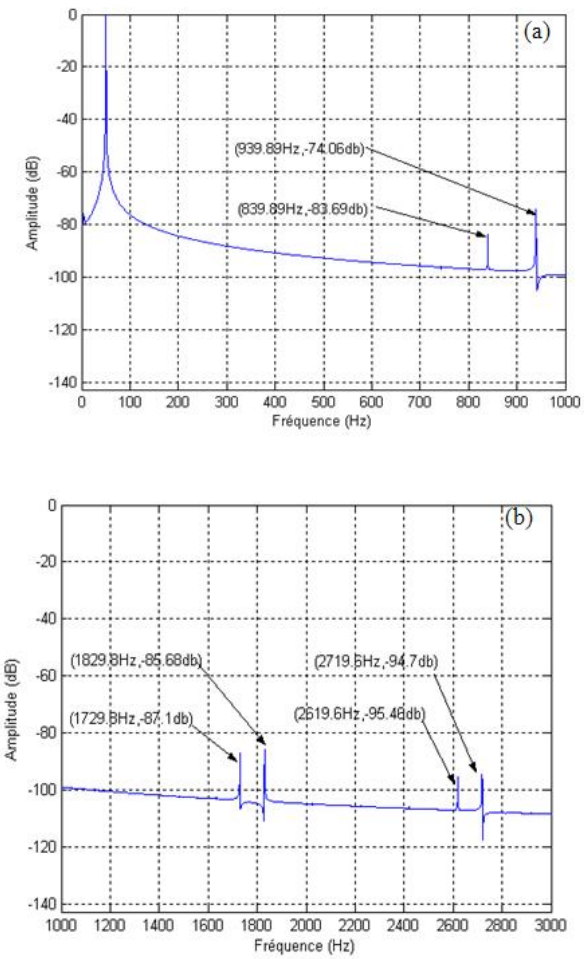

Fig. 7 The phase A stator current spectrum with taking into account the inclination of the bars, (a) for low frequencies order, (b) for high frequencies order

REFERENCES

[1] X. Liang ILochonwu. O, "Induction Motor starting in Practical Industrial Applications", IEEE *Trans. Ind. App, vol. 47*, pp. 271-280, 2011.

[2] A. Anugrah, R. Omar, M. Sulaiman and A. Ahmad, "Fuzzy Optimization for Speed Controller of an Indirect Vector Controlled Induction Motor Drive using Matlab Simulink", JATIT*, vol. 28*, no.2, June 2011.

[3] I. P. Georgakopoulos, E. D. Mitronikas and A. N. Safacas, "Detection of Induction Motor Fault in Inverter Drives Using Inverter Input Current Analysis", IEEE *Trans. Ind. Electronics, vol. 58*, pp. 4365-4373, Sep.2011.

[4] A. Braham and Z. Lachiri, "Diagnosis of Broken Bar Fault in Induction Machines Using Advanced Digital Signal Processing", IREE, vol.5, pp. 1460-1468, July-August.2010.

[5] S. Laribi and A. Bendiabdellah, "Stator Short Circuit And Broken Bar Faults Diagnosis Of An Indirect Vector Control Squirrel Cage Induction Motor, IREE, vol.5, pp. 2088-2094, September-October.2010.

[6] A. Chaouch and A. Bendiabdellah, "Mixed Eccentricity Fault Diagnosis in Saturated Squirrel Cage Induction Motor", International Review on Modelling and simulations (IREMOS), Vol. 5, No. 3, pp.1216-1223, 2012.

[7] A. Bendiabdellah, N. Benouzza, D. Toumi. "Cage motor faults detection algorithme using speed estimation and current analysis", 3rd IEE International Conference PEMD, 2006, pp 47-51, Dublin, Ireland.

[8] M. G. Joksimovic, D. M. Durovic and A. B. Obradovic, "Skew and Linear Rise of MMF Across Slot Modeling-Winding Function Approach". IEEE Transactions on Energy Conversion , Vol. 14, no. 3, pp. 315-320, Sept.1999.

[9] G. Bossio, C. De Angelo, J. Solsona, G. García and M. I. Valla, "A 2D-Model of the Induction Motor: An Extension of the Modified Winding Function Approach", 28th Annual Conference of the IEEE Industrial Electronics Society IECON 2002 , Sevilla Spain, 5-8 Nov. 2002.

[10] G. Bossio, C. De Angelo, J. Solsona y G. García, "Modeling of Induction Machines with Axial Non Uniformity", Congresso Basileiro de Electrônica de Potência, COBEP´2001 , Vol.2, pp 630-634. Florianópolis, Brasil, 2001.

[11] A. Barbour and W. T. Thomson, "Finite Element Study of Rotor Slots Design with Respect to Current Monitoring for Detecting Static Air-Gap Eccentricity in Squirrel-Cage Induction Motor", Proceedings of the IEEE-IAS Annual Meeting Conference, New Orleans, LA, Oct. 5-9, 1997, pp. 112-119.

[12] S. Williamson, T. Flack and A. Voschenk, "Representation of Skew in Time_Stepped Two-Dimensional Finite Element Models of Electrical Machines", IEEE Transactions on Industry Applications, Vol. 31, No. 5, pp. 1009-1015, 1995.

[13] C. McClay and S. Williamson, "The Variation of Cage Motor Losses with Skew" , IEEE Transactions on Industry Applications, Vol. 36, No. 6, pp. 1563-1570, 2000.

[14] G. Barakat, G. Houdouin, B. Dakyo and E. Destobbeleer, "An Improved Method for Dynamic Simulation of Air-Gap Eccentricity in Induction Machines", IEEE Sdemped 2001, pp. 133- 138.

[15] G. Bossio, C. De Angelo, J. Solsona, G. García and M. I. Valla, "A 2DModel of the Induction Motor: An Extension of the Modified Winding Function Approach", 28th Annual Conference of the IEEE Industrial Electronics Society IECON 2002 , Sevilla Spain, 5-8 Nov. 2002.

Azeddine Bendiabdellah is born in Saida Algeria in 1958. He received his Bachelor Engineering degree with honors and his Ph.D degree from the University of Sheffield, England, in 1980, and 1985 respectively. From 1990 to 1991 he was a visiting professor at Tokyo Institute of Technology (T.I.T), Japan. He is currently Professor of Electrical Engineering at the University of Sciences and Technology of Oran, (USTO) Algeria. His research interests include: Electrical Machines & Drives Analysis and Modeling, Electrical Machines & Drives Control, Electrical Machines & Drives Faults Diagnosis.

Abdellah Chaouch is born in Mostaganem Algeria in 1971. He received his Engineering, Magister and Doctoral degree from University of Sciences and Technology of Oran, (USTO) Algeria.. He is currently a teacher of Electrical Engineering at the University of Mostaganem, Algeria. email: ikchaouchdz@yahoo.fr